

HIGH-RESOLUTION SIMULATIONS OF THE FINAL ASSEMBLY OF EARTH-LIKE PLANETS 2: WATER DELIVERY
AND PLANETARY HABITABILITYSEAN N. RAYMOND^{1,2}, THOMAS QUINN¹, & JONATHAN I. LUNINE³*Draft version February 3, 2019*

ABSTRACT

The water content and habitability of terrestrial planets are determined during their final assembly, from \sim 1000-km “planetary embryos” and a swarm of billions of 1-10 km “planetesimals.” During this process, water-rich material is accreted by terrestrial planets via impacts of water-rich bodies originating beyond roughly 2.5 AU. We present analysis of water delivery and habitability in five high-resolution simulations of terrestrial accretion first described in Raymond, Quinn & Lunine (2006 – *Icarus*, submitted).

In five simulations, we have formed a total of 15 terrestrial planets, including five potentially habitable planets. Each simulation formed 2-4 planets with masses from 0.4 to 2.6 Earth masses. Every planet from each simulation accreted at least the Earth’s current water budget; most accreted several times that amount (assuming no impact depletion). Each planet accreted at least five water-rich embryos and planetesimals from past 2.5 AU; most accreted 10-20 water-rich bodies. We show that the process of water delivery to Earth-like planets is less stochastic than previously thought. Terrestrial planets accrete a large number of water-rich planetesimals in a statistically robust way, and a few water-rich embryos in a stochastic, “hit or miss” process.

In one interesting case, two \sim Earth-mass, potentially habitable planets formed in one system, at the inner and outer edges of the habitable zone. The eccentricities of both planets oscillate out of phase, with amplitudes of \sim 0.2. At certain times, their eccentric orbits cause each planet’s orbit to venture either interior or exterior to the habitable zone.

Subject headings: planetary formation – water delivery – extrasolar planets – cosmochemistry

1. INTRODUCTION

The last stages of terrestrial accretion consist of the agglomeration of a swarm of trillions of km-sized planetesimals into a few massive planets (see Lissauer, 1993, for a review). This process determines the orbit, mass, and water content of terrestrial planets. These properties, in turn, determine the possibility that such planets may be capable of supporting life.

What characteristics define a habitable planet? If the Earth is a good representation, then it appears that a habitable planet must satisfy several important criteria: 1) It must have a significant mass – Williams *et al.* (1997) found a minimum mass of 0.23 Earth masses (M_{\oplus}); 2) It must orbit its star in the “habitable zone”: it must have the right temperature to support liquid water on its surface (Kasting *et al.* 1993); and 3) It must have an appreciable water budget – a dry planet in the habitable zone is not likely to be habitable.

Morbidelli *et al.* (2000) proposed that most of the Earth’s water was accreted from one or two water-rich embryos from the outer asteroid region, beyond roughly 2.5 AU. In this model, the water content of protoplanets⁴ in the habitable zone is very small, so an external source of water is needed (but see Drake & Righter, 2002, for a differing opinion). A single water-rich embryo contains more than the Earth’s entire water budget, so the number of impacts of such embryos must have been very small. In the model of Morbidelli *et al.* (2000), water delivery is therefore a highly stochastic, “hit or miss” process. Small number statistics suggest that many Earth-like planets may form in the habitable zone but not accrete any water-rich embryos. Such

planets have been formed in low-resolution simulations (Raymond *et al.* 2004 – hereafter RQL04), and are likely to be dry and inhospitable to life.

Previous dynamical simulations have shown that terrestrial planets may form with a range in mass and water content (Wetherill 1996; Morbidelli *et al.* 2000; Chambers & Cassen 2002; RQL04; Raymond *et al.* 2004, 2005a, 2005b). Although these simulations typically started from only 20-200 particles, they did establish certain trends relating to planetary habitability: 1) The eccentricity of the giant planets has a strong effect on the water content of the terrestrial planets (Chambers & Cassen 2002; RQL04). An eccentric giant planet preferentially ejects water-rich material beyond 2-3 AU, causing the terrestrial planets to be relatively dry. 2) An increase in either the giant planet mass or the surface density of solid material results in the formation of a smaller number of more massive terrestrial planets. With fewer planets forming, the chances that a given planet will lie in the habitable zone is reduced.

In this paper, we focus on 1) the efficiency and stochasticity of water delivery, and 2) habitability of terrestrial planets. We analyze the outcome of five high-resolution simulations from Raymond *et al.* (2006; hereafter Paper 1), containing between 1000 and 2000 initial particles. For the first time, these simulations directly simulate a realistic number of embryos according to various models of their formation. Our simulations were designed to examine the accretion and water delivery processes in more detail, and also to explore the dynamical effects of including a larger number of particles than in previous simulations.

¹Department of Astronomy, University of Washington, Box 351580, Seattle, WA 98195 (raymond@astro.washington.edu)²Current address: Laboratory for Atmospheric and Space Physics, University of Colorado, Boulder, CO 80309³Lunar and Planetary Laboratory, The University of Arizona, Tucson, AZ 85287.⁴We use the term protoplanets to refer to all terrestrial building blocks, including both planetesimals and planetary embryos. This departs from certain previous uses of the term, which use protoplanets as a synonym of planetary embryos.

Section 2 briefly summarizes the simulations from Paper 1. Section 3 discusses the delivery of water-rich material to the terrestrial planets, including a discussion of the stochasticity of the process. Section 4 explores the physical properties and potential habitability of the planets formed in each simulation. Section 5 summarizes our new results and concludes the paper.

2. DESCRIPTION OF SIMULATIONS

Our dataset consists of the five simulations from Paper 1, which were started from three sets of initial conditions. Each system includes a Jupiter-mass planet on a circular orbit at 5.2–5.5 AU (hereafter simply referred to as “Jupiter”), and starts from a disk of 1000–2000 protoplanets on low-eccentricity and low-inclination orbits between 0.5 and 5 AU. Note that our starting number of particles is ~ 5 –10 times larger than in previous work.

- Simulation 0 starts in the late stages of oligarchic growth, when planetary embryos were not yet fully formed. It contains a total of 1885 sub-isolation mass bodies.
- Simulation 1 follows the results of Kokubo & Ida (2000), who suggest that the timescale for the formation of planetary embryos is a function of heliocentric distance. Interior to the 3:1 resonance with Jupiter at 2.5 AU we include embryos. Exterior to the 3:1 resonance, we divide the total mass into 1000 planetesimals with masses of $0.006 M_{\oplus}$.
- Simulation 2 assumes that planetary embryos formed all the way out to 5 AU. However, a significant component (roughly one third) of the total mass is still contained in a swarm of planetesimals which are littered throughout the region.

For simulations 1 and 2, we perform two runs varying the numerical treatment of planetesimals: a) In simulations 1a and 2a all bodies interact with each other; b) in simulations 1b and 2b the “planetesimals” are not self-interacting. They gravitationally interact with embryos and with Jupiter, but not with each other. This allows for significant computational speedup. Each simulation was evolved for ≥ 200 Myr with the hybrid integrator in *Mercury* (Chambers 1999).

Our sets of starting conditions may correspond to either different timescales for the formation of Jupiter, or different timescales for embryo formation (see Paper 1 for more detail). The more important distinction is the timescale for embryos to form in the region from 2–5 AU: the simulations of Kokubo & Ida (2000, 2002) suggest that embryos form slowly in this region, while Goldreich *et al.* (2004) calculate a much faster timescale for embryo growth.

The initial water content of protoplanets is designed to reproduce the water content of chondritic classes of meteorites (see Fig. 2 from RQL04): inside 2 AU bodies are initially dry; outside of 2.5 AU they have an initial water content of 5% by mass; and between 2 and 2.5 AU they contain 0.1% water by mass. The starting iron contents of protoplanets are interpolated between the values for the planets (neglecting Mercury) and chondritic classes of meteorites, with values taken from Lodders & Fegley (1998), as in Raymond *et al.* (2005a, 2005b). To span our range of initial conditions, we interpolate to values of 0.5 at 0.2 AU and 0.15 at 5 AU.

⁵Note that the noble gas ratios in the Earth’s atmosphere are not consistent with those in asteroidal material; however, this is explained by a dual source of Earth’s atmosphere – a mixture of nebular and chondritic components (Genda & Abe 05).

Fifteen terrestrial planets formed in these five simulations, including five potentially habitable planets. The properties of these planets are shown in Table 1 (reproduced from Paper 1), and discussed in detail below.

3. WATER DELIVERY TO TERRESTRIAL PLANETS

Here we describe in detail the acquisition of water by terrestrial planets. We assume that protoplanets formed at 1 AU are dry (in contrast to Drake & Righter 2002), and that the water content of chondritic classes of meteorites is representative of the starting water content of protoplanetary disks.

In section 3.1 we summarize the sources and timescales for water delivery to terrestrial planets, including comets. In section 3.2 we discuss the efficiency of the delivery of water-rich material from the outer asteroid region. In section 3.3 we discuss the mass distribution of water-bearing impactors, with consequences for the robustness/stochasticity of the water delivery process. In section 3.4 we discuss the retention of water during collisions.

3.1. Summary of sources of water and delivery timescales

In the simulations presented here, we only consider the outer asteroid region as a source of water. However, the Earth (and other terrestrial planets) likely accreted water-rich material from several sources at different times:

1. Icy planetesimals in the Jupiter-Saturn region have dynamical lifetimes of only $\sim 10^5$ years and Earth-collision probabilities of only $\sim 10^{-6}$ (Morbidelli *et al.* 2000), so these impacted the terrestrial planets very early in their formation. If Jupiter formed quickly, most of this water was likely lost due to the planets’ small masses (and therefore low surface gravities). However, if Jupiter formed late, Jupiter-Saturn comets could have contributed a small fraction of Earth’s water (Morbidelli *et al.* 2000).
2. During accretion, water-rich planetesimals and embryos from the outer asteroid region between 2.5–4 AU were incorporated into the planets, delivering the bulk of Earth’s water. This is the source of water considered here.
3. After accretion, icy comets from beyond Neptune’s orbit were scattered into the inner Solar System. The “late heavy bombardment” of comets occurred roughly 700 million years after the terrestrial planets formed (e.g. Gomes *et al.* 2005). A comparison of the D/H ratio in Earth water and comets suggests that these contributed less than 10% to the Earth’s water budget⁵ (Morbidelli *et al.* 2000).
4. The Earth continues to be impacted at a low rate by water-rich asteroids and comets.

3.2. Source regions and efficiency of water delivery

Figure 1 (top panel) shows the fraction of water-rich material delivered to the surviving terrestrial planets as a function of starting semimajor axis. The region from 2–5 AU is divided into six bins, each with a width of 0.5 AU (i.e., 2–2.5 AU, 2.5–3 AU, etc). We only consider water delivery to planets inside 2 AU, thereby excluding planet *d* from simulation 2a. It is clearly

TABLE 1
PROPERTIES OF (potentially habitable) PLANETS FORMED¹

Simulation	Planet	a (AU)	e^2	$i(^{\circ})$ ³	$M(M_{\oplus})$	W.M.F.	N(oceans) ⁴	Fe M.F.
0	a	0.55	0.05	2.8	1.54	2.6×10^{-3}	15	0.32
	b	0.98	0.04	2.4	2.04	8.4×10^{-3}	66	0.28
	c	1.93	0.06	4.6	0.95	9.1×10^{-3}	33	0.28
1a	a	0.58	0.05	2.7	0.93	8.3×10^{-3}	30	0.31
	b	1.09	0.07	4.1	0.78	5.5×10^{-3}	17	0.30
	c	1.54	0.04	2.6	1.62	1.2×10^{-2}	75	0.26
1b	a	0.52	0.06	8.9	0.60	7.2×10^{-3}	17	0.31
	b	1.12	0.05	3.5	2.29	6.7×10^{-3}	60	0.29
	c	1.95	0.09	9.7	0.41	3.8×10^{-3}	6	0.28
2a	a	0.55	0.08	2.6	1.31	9.3×10^{-4}	5	0.33
	b	0.94	0.13	3.4	0.87	8.6×10^{-3}	29	0.29
	c	1.39	0.11	2.4	1.46	6×10^{-3}	34	0.29
2b	a	0.61	0.18	13.1	2.60	1.8×10^{-2}	75	0.24
	b	1.72	0.17	0.5	1.63	7.1×10^{-3}	71	0.30
							126	0.22
Mercury ⁵		0.39	0.19	7.0	0.06	1×10^{-5}	0	0.68
Venus		0.72	0.03	3.4	0.82	5×10^{-4}	1.5	0.33
Earth		1.0	0.03	0.0	1.0	1×10^{-3}	4	0.34
Mars		1.52	0.08	1.9	0.11	2×10^{-4}	0.1	0.29

¹Planets are defined to be $> 0.2 M_{\oplus}$. Shown in bold are bodies in the habitable zone, defined to be between 0.9 and 1.4 AU. This is slightly wider than the habitable zone of Kasting *et al.* (1993).

²Mean eccentricity averaged during the last 50 Myr of the simulation.

³Mean inclination averaged during the last 50 Myr of the simulation.

⁴Amount of planetary water in units of Earth oceans, where 1 ocean = 1.5×10^{24} ($\approx 2.6 \times 10^{-4} M_{\oplus}$).

⁵Orbital values for the Solar system planets are 3 Myr averaged values from Quinn *et al.* (1991). Water contents are from Morbidelli *et al.* (2000). Iron values are from Lodders & Fegley (1998). The Earth's water content lies between 1 and 10 oceans – here we assume a value of 4 oceans. See text for discussion.

easiest to deliver water to the terrestrial planets from the innermost water-rich region, between 2 and 2.5 AU. The efficiency of water delivery drops off at higher orbital distances, because (i) bodies are physically more distant, and need to travel greater distances to impact the terrestrial planets, and (ii) Jupiter's dynamical effects cause many outer asteroid bodies to be ejected before they may be accreted onto the terrestrial planets. The efficiency of water delivery is similar for most simulations, with typical mid-asteroid region values between 5 and 20%. The efficiency of water delivery in simulation 2b is very high, with values above 20% out to 4 AU. Simulation 2a has the lowest values, because water delivery to planet *d* at 2.19 AU has not been accounted for. Planet *d* acts as a small dynamical barrier for inward-diffusing bodies, and also accretes much of its local, water-rich material.

Figure 1 (bottom panel) shows the quantity of water delivered to the terrestrial planets from each bin between 2 and 5 AU for each simulation. Again, this only includes planets inside 2 AU, which excludes planet *d* from simulation 2a. The shape of the curves mirror those in the top panel, except for the first point that represents water delivery from 2-2.5 AU. The water content of this region is much lower than past 2.5 AU (0.1% vs. 5%), so the region simply does not contain much water. The total starting water content between 2-2.5 AU is about 3 oceans in each simulation. The major source of water for terrestrial planet lies between 2.5 and 4 AU. Inside 2.5 AU, bodies don't start with enough water, and past 4 AU the dynamical lifetime of bodies is too short to deliver water. Indeed, the vast majority of material exterior to the 3:2 mean-motion resonance with Jupiter is destroyed via collisions with or ejections by Jupiter in the first 10^{4-5} years of each simulation.

Figure 2 shows the water mass fraction of each terrestrial planet in our five simulations as a function of the planet's final mass. The size of each body is proportional to its relative physical size, and the color corresponds to its water mass fraction, as shown in the color bar. Higher-mass planets do not necessarily have higher water contents than lower-mass ones. Indeed, Fig. 2 is more or less a scatter plot. Almost all planets have water mass fractions between 3×10^{-3} and 2×10^{-2} . As shown in RQL04, water mass fraction is a function of the planets' orbital distance: planets with orbital radii inside 1 AU accrete systematically less water. The four planets with water mass fractions less than 3×10^{-3} all have $a \leq 1$ AU. The water content of the planets formed in these simulations is a stronger function of orbital distance than of planetary mass.

3.3. Stochasticity of water delivery

The size distribution of water-bearing impactors is important for the robustness/stochasticity of the water delivery process, as well as for volatile retention during collisions. We have the resolution in these simulations to discriminate between planetary embryos and planetesimals, although our planetesimals are still many orders of magnitude larger than realistic values.

Fig. 3 shows the timing of all impacts which built up the three planets from simulation 0, color-coded by planet. Water-rich bodies were not accreted by the planets in simulation 0 until ~ 10 Myr after the start of the simulation. Planet *a* accreted 14 bodies with non-zero water contents, and incorporated a total of 18 bodies from past 2 AU totaling $0.12 M_{\oplus}$. Only one water-rich body accreted by planet *a* was an embryo, with mass of $0.48 M_{\oplus}$. This protoplanet collided with planet *a* at $t = 21$ Myr, and can be seen as a large step in mass in Figure 4 from Pa-

per 1 (note that planet *a* also accreted a dry, $0.25 M_{\oplus}$ embryo at 20.6 Myr). This embryo contained only a small amount of water in the form of three protoplanets from between 2 and 2.5 AU, totaling about 1 Earth ocean. The majority of the water accreted by planet *a*, totaling 15 oceans, was in the form of several smaller protoplanets from past 2-2.5 AU which had accreted 0-2 other protoplanets. These were accreted by planet *a* at preferentially later times, after the accretion of the embryo.

The situation is different for planets *b* and *c*. Planet *b* accreted 24 bodies from past 2 AU, comprised of a total of 60 water-rich protoplanets carrying 66 oceans of water. Five of these 24 water-delivering bodies were embryos, which delivered over half of planet *b*'s water inventory, 37 out of 66 oceans of water. Planet *c* accreted 12 bodies from past 2 AU comprised of 39 water-rich protoplanets. Three of the twelve impactors were embryos, which delivered 69% of planet *c*'s total water, 23 of its 33 oceans.

It is interesting that the size distribution of water-bearing impactors differs for planet *a* and planets *b* and *c*. Previous simulations including only planetary embryos in the asteroid belt have concluded that the water delivery process from that region is highly stochastic (Morbidelli *et al.*, 2000; RQL04). As only a small number of embryos ($\sim 20-50$) were included in the region, variations from simulation to simulation might drastically change the water content of the terrestrial planets that form. The addition of small bodies changes the stochastic aspect of water delivery.

Indeed, previous work has characterized the water delivery process as being very stochastic, i.e. a “hit or miss” process (Morbidelli *et al.*, 2000; RQL04). This is largely due to computational limitations, which necessitated the assumption that all mass in the outer asteroid region is in the form of planetary embryos. However, in an embryo-dominated scenario, only one water-rich embryo is needed to deliver the Earth's (current) water budget. There are also isotopic constraints that limit the total amount of carbonaceous chondritic material accreted by the Earth to be only a few percent of its total mass (Drake & Righter, 2002). It is therefore often assumed that the Earth accreted only 1-2 water-rich embryos. In the context of planets forming around other stars, small-numbers statistics suggests that a significant fraction of Earth-like planets will be devoid of water (at least from an asteroidal source).

Each planet in our five high-resolution simulations accreted at least 5 water-rich bodies; most accreted more than 10. Table 2 shows the water content of each planet, as well as the number of water-rich impactors, and fraction of water delivered in the form of large bodies (embryos) vs. small bodies (planetesimals). Since our planetesimals are much larger than realistic, 1 km planetesimals, we must be careful in our definition of “small bodies”. This distinction is only needed for simulations 0 and 1a, as in the other cases water-rich embryos are either pre-formed (simulations 2a, 2b) or cannot themselves accrete (simulation 1b). The smallest planetary embryos that form given a typical spacing of 5-10 mutual Hill radii are $0.03-0.05 M_{\oplus}$, in the very inner part of the disk. Embryos past 2 AU can range from 0.07 to almost $0.2 M_{\oplus}$, depending on the spacing. We define a planetary embryo to be a body that is at least $0.05 M_{\oplus}$, or is an agglomeration of at least four smaller bodies. There still exists a continuum in the mass range of water-bearing bodies, ranging from planetesimals which have not accreted any other bodies to Moon-sized accumulations of 2-3 planetesimals.

Figure 4 shows the amount of water delivered to the terres-

trial planets in each impact, color-coded by simulation. The size of each body represents the relative physical size of each impactor. The amount of water per planetesimal in simulations 1a and 1b, ~ 1.2 oceans, is immediately evident. There clearly exists a range in the volume of water delivered during these impacts. The size of the impactor does not always correlate with the amount of water delivered. In some cases, large embryos either accrete one or two water-rich planetesimals, or perhaps form in the “slush” region between 2 and 2.5 AU. These large bodies may therefore deliver only a very small amount of water. In general, however, larger impactors deliver more water, as they usually contain many water-rich planetesimals.

Every planet in each of our simulations has accreted a significant amount of material from past the snow line, and been delivered at least 6 oceans of water. The innermost planets in simulations 0 and 1b received most of their water from planetesimals, while planets in the habitable zone and exterior received a larger amount of water from embryos. Even in simulation 2b, in which the embryo mass is twice the planetesimal mass, 2-3 oceans of water is delivered to each planet in the form of planetesimals.

The masses of embryos in these simulations are consistent with models of oligarchic growth (e.g., Kokubo & Ida 2000, 2002). However, the mass of each “planetesimal” is $10^{-3} - 10^{-2} M_{\oplus}$, much larger than expected for standard, ~ 1 km planetesimals. If each planetesimal represents a large number of much smaller bodies whose dynamical effects we cannot account for, then a simple mass-scaling argument demonstrates that one $0.01 M_{\oplus}$ planetesimal is equivalent to about 10^9 realistic, km-sized bodies. If the accretion process proceeds in the same way, we would expect that each terrestrial planet to accretes a few water-rich embryos and billions of water-rich planetesimals. However, such a claim would be overstating our results, which show that Earth-like planets in the habitable zone are likely to accrete *at least* 10-20 water-rich bodies of significant mass.

The effective Poisson noise from the 1-2 water-delivering embryos is the reason for the previous result that water delivery is highly stochastic, a “hit or miss” process. Our results suggest at least an order of magnitude increase in the number of water-bearing bodies. The Poisson noise is therefore substantially reduced, implying that this is a more robust process than previously thought. A conservative interpretation of our results suggests that stochastic variations in the water content of planets exist at the $\sim 20\%$ level.

Chance fluctuations between similar protoplanetary systems will create a range in water content, but this range is much smaller than previously thought (Morbidelli *et al.* 2000; RQL04). For protoplanetary systems like those we have modeled, we therefore expect a baseline water content of roughly 5-20 oceans (pre-depletion) to be accreted in the form of planetesimals from past the snow line. On top of this, a small number of water-rich embryos may be accreted.

Fig. 3 shows that water-delivering impacts do not occur in simulation 0 until at least 10 Myr, at which point planets are likely to have reached a substantial fraction of their final mass and have primitive atmospheres. However, Fig. 4 shows that water-bearing impacts happen earlier in the other simulations. As discussed above, a given annulus remains dynamically isolated until it can grow bodies of a significant size, capable of scattering material out of the region. Simulation 0 was the only case in which we allowed this process to occur throughout the

TABLE 2
WATER DELIVERY TO (potentially habitable) PLANETS¹

Sim.-planet	$a(AU)$	$M(M_{\oplus})$	N(oceans)	H ₂ O impacts (total) ²	Embs (pl/ls) ³	%H ₂ O(emb) ⁴	Pl/I Oceans ⁵
0-a	0.55	1.54	15	14 (18)	1 (13)	0.07	14
0-b	0.98	2.04	66	24 (60)	7 (17)	0.60	26
0-c	1.93	0.95	33	12 (39)	3 (9)	0.69	10
1a-a	0.58	0.93	30	14 (25)	2 (12)	0.48	16
1a-b	1.09	0.78	17	7 (14)	1 (6)	0.43	10
1a-c	1.54	1.62	75	22 (64)	4 (18)	0.54	35
1b-a	0.52	0.60	17	10 (14)	1 (9)	0.35	11
1b-b	1.12	2.29	60	24 (52)	7 (17)	0.66	20
1b-c	1.95	0.41	6	5 (5)	1 (4)	0.20	5
2a-a	0.55	1.31	5	13 (16)	1 (12)	0.12	4
2a-b	0.94	0.87	29	8 (10)	1 (7)	0.94	2
2a-c	1.39	1.46	34	11 (13)	3 (8)	0.98	1
2a-d	2.19	1.08	75	9 (12)	4 (5)	0.96	3
2b-a	0.61	2.60	71	9 (24)	2 (7)	0.96	3
2b-c	1.72	1.63	126	11 (24)	3 (8)	0.98	3
Earth⁶	1.0	1.0	1-10	?	?	?	?

¹ Shown in bold are bodies in the habitable zone, between 0.9 and 1.4 AU.

² Number of water-delivering impacts. Shown in parentheses is the total number of bodies incorporated in these impacts from past 2 AU.

³ Number of water-bearing planetary embryos, defined to be at least 0.05 M_{\oplus} . Shown in parentheses is the number of water-bearing planetesimals.

⁴ Fraction of the total water content delivered in the form of large bodies (embryos).

⁵ Number of oceans of water delivered to the planet in the form of planetesimals.

⁶The amount of water in Earth's mantle is highly uncertain – see Morbidelli *et al.* (2000) for a discussion.

disk, and it displayed the expected, outward-moving trend. We therefore consider the trend in Fig. 3 to be our most accurate representation of accretion through time.

Water-rich embryos are preferentially accreted by more massive planets and by planets at larger orbital radii. The path of a water-rich body from past the snow line to the terrestrial region involves an inward diffusion via multiple encounters with other bodies. The probability of such a body being accreted depends on the body's cross section for impact as well as the accreting body's cross section (i.e., its mass). The cross section of planetesimals is small, so the impact probability depends only on the cross section and orbit of the accreting body. More massive planets naturally accrete more water-rich material than less massive ones. Planets at larger orbital radii are simply closer to the source of water-rich planetesimals, and have a higher number of encounters than planets closer to the Sun. The impact cross section of embryos which either originated past the snow line or accreted smaller, water-rich bodies is not negligible. The probability of accretion during inward diffusion depends on the embryo mass as well as the planet mass. Therefore, embryos are more likely than planetesimals to be accreted by massive planets and by planets at larger orbital radii.

Morbidelli *et al.* (2000) derived an impact probability of $10^{-(3-4)}$ for water-rich asteroids (planetesimals) in the presence of embryos. They also found that water-rich embryos were accreted at a later time than water-rich planetesimals. Two of our five simulations (sims. 2a and 2b) have starting conditions similar to previous models, allowing us to test previous results. In particular, Morbidelli *et al.* (2000) treated small bodies as test particles, so we can compare their results with the outcome of simulation 2b, and test them against the results of the fully-interacting bodies in simulation 2a.

A simple change in the way that planetesimals are numerically treated appears to have a qualitative effect on the timing of the accretion of water-rich planetesimals and embryos.

Large, water-rich embryos scatter planetesimals in simulations 2a and 2b onto unstable orbits, quickly lowering their number. However, many planetesimals still diffuse inward and collide with the terrestrial planets. In simulation 2a, water-rich embryos and planetesimals are accreted concurrently, but planetesimal impacts continue to later times, in contrast to Morbidelli *et al.* (2000). Five out of 17 (29%) water-rich planetary embryos and 35 of 521 (7%) water-rich planetesimals were incorporated in the final planets as small bodies, although 11 additional planetesimals were accreted by embryos before impacting the forming planets. Water delivery efficiencies are quite different in sim. 2b – more than half of water-rich embryos (59%) ended up in planets, but only 3% of planetesimals were accreted by the planets as small bodies (an additional 5% of planetesimals were accreted by embryos, and then by the planets). This simulation agrees with Morbidelli *et al.* (2000) in that water-rich embryos are accreted after water-rich planetesimals. It is interesting, however, that in the more realistic, fully self-interacting simulation 2a, water-rich planetesimals are accreted to later times than embryos.

The fraction of total water accreted by the planets in simulations 2a and 2b is far higher than in our 3 other simulations. Indeed, each planet but one (planet *a* from simulation 2a) received $> 90\%$ of its water in the accretion of embryos. Nonetheless, each planet in simulations 2a and 2b accreted at least one ocean of water from at least five water-rich planetesimals; most accreted about three oceans from small bodies. We began our simulations with roughly two thirds of the mass in the form of embryos, although oligarchic growth should end when half of the mass is in large bodies. In addition, since embryos are thought to grow more slowly at larger heliocentric distances (Kokubo & Ida 2000), the fraction of the total water-rich mass in the form of planetesimals may be even higher.

If we assume more initial mass in the outer regions to be in the form of planetesimals, the amount of water delivered by

these small bodies increases correspondingly. The increase is likely to be super-linear, because the dynamical presence of embryos in the region is the main destruction mechanism of planetesimals. A simple factor of two increase in the total mass in planetesimals (vs. embryos) is likely to cause all planets to accrete a minimum of 3 oceans of water in the form of planetesimals.

Our results suggest that understanding the true mass distribution of the disk at the time of giant planet formation is key to the stochasticity of water delivery. If giant planets form relatively early, or if planetary embryos form slowly (as in Kokubo & Ida 2000), then the outer asteroid region is dominated by small bodies. Our results from simulations 0 and 1a suggest that oligarchic growth will be stunted in the asteroid region. Compared with models, fewer water-rich embryos will form, and their masses will be smaller. Over the course of terrestrial accretion, the role of small bodies in water delivery will be comparable to that of embryos. As a result, there is a large number of water-bearing impactors, and water delivery to the planets is robust.

However, if giant planets form *very* late, or if planetary embryos form very quickly (as in Goldreich *et al.* 2004), then the mass distribution in the asteroid region is dominated by embryos. Thus, water is delivered by a small number of impactors. Water delivery in this context is therefore stochastic, but less so than in previous models (Morbidelli *et al.* 2000; RQL04) because a few oceans of water are still delivered by small bodies.

It is unclear which of the above scenarios is accurate. In other words, the mass distribution in the asteroid region at the time of giant planet formation is uncertain. Giant planets are constrained to form within the first few million years of the disk, because this is the timescale for the dissipation of the gas disk (Briceño *et al.* 2001). Whether giant planets form via core-accretion (Pollack *et al.* 1996) or gravitational instability (Boss 1997) is not important, unless it happens within $\sim 10^5$ years (which is possible only via collapse). A giant planet at 5.2 AU does not affect embryo formation inside roughly 2-2.5 AU. The remaining issue is the timescale for embryo formation in the asteroid region. Kokubo & Ida (2000) suggest that embryos form slowly, requiring ~ 10 Myr to form at 2.5 AU. In contrast, Goldreich *et al.* (2004) calculate analytically that dynamical friction generated by a collisional cascade reduces this timescale to 10^5 years or less throughout the inner disk. Weidenschilling *et al.* (1997) simulated this process and found a timescale of $\sim 10^5$ years for embryos to grow at 1 AU, roughly 10 times shorter than the results of Kokubo & Ida (2000), but slower than Goldreich *et al.* (2004). However, Leinhardt & Richardson (2005) find that embryos grow in the manner suggested by Kokubo & Ida, while accounting for both fragmentation during collisions and dynamical friction from remnant small bodies below their resolution limit. This issue clearly remains unresolved, although its importance for the stochasticity of water delivery is significant.

3.4. Retention of water during accretion

If a planet has an atmosphere, then the explosion generated by the impact of a planetesimal-sized body is confined and very little material escapes (Sleep & Zahnle 1998). In the absence of an atmosphere, the volatile retention of the impact of a planetesimal-sized body is largely determined by the impact velocity and the planet's escape velocity (Sleep & Zahnle, 1998; Segura *et al.*, 2002). Late stage, water-rich planetesimal impacts have typical velocities of only a few km s^{-1} more than the

escape speed of the accreting body. In this velocity range, we expect impacting bodies and their volatiles to be preserved on the accreting planets. Thus, virtually all water delivered in the form of planetesimals is retained.

A collision between an Earth-sized planet and a Mars-sized body will typically erode 30% of the larger planet's atmosphere and 10% of the smaller planet's atmosphere (Genda & Abe 2003). A key factor in the retention of the planet's atmosphere and ocean in a giant impact is the ground velocity induced by the impact shock. Genda & Abe (2005) have shown that the presence of an ocean greatly affects a planet's ability to retain an atmosphere or the oceans themselves. The shock impedance of an ocean is less than for a planetary surface, so the ground velocity during an impact on an ocean-covered world is higher, as is the escape fraction. The highly energetic vapor injected from the oceans into the atmosphere during an impact imparts energy to the atmosphere, which may exceed the escape velocity and leave the planet (Genda & Abe 2005; Zahnle 2005). Only when the atmosphere is destroyed can water be lost from the planet's surface (Genda & Abe 2005).

Water delivered to the planets in the form of small, planetesimal-sized bodies is likely to be retained by the planets. Water delivered by planetary embryos may be lost or retained, depending on the details of the collision (e.g. Genda & Abe 2005), but this process remains relatively poorly understood. This discrepancy between almost certain water retention for small, water-rich impactors and an uncertain outcome for embryo-sized, water-bearing impactors implies that large fraction of water on planetary surfaces may have its origin in small bodies.

In addition, the time dependence of water-delivering impactors seen in Fig. 3 implies that the planets' water retention may also be a function of time. The earliest water-delivering bodies encounter dry planets with strong impedance to the impact-generated shock wave. Later water-bearing bodies impact possibly ocean-covered worlds, and may lead to reduced atmospheric and water retention (Genda & Abe, 2005).

4. PHYSICAL PROPERTIES AND HABITABILITY OF PLANETS

The five high resolution simulations presented here have formed a total of 15 terrestrial planets more massive than 0.2 M_\oplus : 14 of these have semimajor axes inside 2 AU, and five lie in a broadly-defined habitable zone between 0.9 and 1.4 AU. All have water contents equal to or higher than the Earth's current water content, before taking volatile loss into account. We have not considered the outer reaches of the planetary system as a source of water (i.e. cometary water); if accretion proceeds as on the Earth, we expect this to contribute $\leq 10\%$ of the total water budget (Morbidelli *et al.*, 2000). The water content of the Earth is disputed – the mantle contains an uncertain 1-10 oceans of water (see Morbidelli *et al.*, 2000, for a discussion), where an ocean is defined as the amount of surface water on the Earth, 1.5×10^{24} grams. In RQL04 and Raymond *et al.* (2005a, 2005b) we assumed the Earth's total current water budget to be 4 oceans, corresponding to a water mass fraction of 10^{-3} .

None of the planets formed have iron contents as high as the Earth's. Planets in the habitable zone typically have iron mass fractions between 0.28 and 0.30, compared with 0.34 for the Earth. This is because the feeding zone of each planet has a significant width, and a significant fraction of each planet's mass originates between 1 and 2.5 AU. The iron mass fraction of bodies in this region is about 0.29. The only region where planets

can accrete material more iron-rich than the Earth is from far inside 0.7 AU, where $FeMF$ is linearly interpolated between Venus' iron content of 0.33 and a dummy value of 0.5 at 0.2 AU (see Section 2). Planets in the habitable zone do not accrete enough of this innermost material to elevate their iron content to the level of Venus and Earth ($FeMF \sim 0.33\text{-}0.34$). This indicates that either our initial conditions are too iron-poor, or that giant impacts during accretion increase the iron content of the planets, in the same way that the Moon-forming impact is thought to have deposited most of its iron into the proto-Earth (e.g., Canup 2004a).

4.1. Determination of physical properties

Table 3 lists the calculated properties for all of the planets formed in our five simulations, as compared with the Solar System terrestrial planets. Figure 5 shows the final configuration of our five simulations, with the Solar system included for scale. The water values in Fig. 5 include a formula for depletion described below.

We assume that planets more massive than the Earth have the same bulk density of the Earth, and planets less massive than the Earth have the same bulk density as Venus. This does not take into account the details of self-compression, but is accurate enough for this exploratory analysis. For example, planet 0-*b*'s (planet *b* from simulation 0) physical radius is $2.04^{1/3} = 1.27$ Earth radii, roughly 8100 km. The iron mass fraction of planet 0-*b* is 0.28, as compared with 0.34 for the Earth. If we assume a simple scaling, the size of planet 0-*b*'s iron core is $(2.04 \times 0.28 / 0.34)^{1/3} = 1.18$ times the size of the Earth's iron core, about 4100 km. The rest of the volume of planet 0-*b* is mantle, with a thickness of 4000 km. Let us assume that the Earth is composed of only a core and a mantle. The mantle therefore comprises 66% of the Earth's mass, 3.8×10^{27} g. If we assume that the mantle contains about 4 oceans of water (slightly more than the 3 oceans assumed above), then we can generalize to assume that the amount of water that may be incorporated into mantle rocks on our simulated planets is 1 ocean per 10^{27} g.

We assume that planets do not retain all of their water. Matsui & Abe (1986) showed that if Earth and Venus had the same starting water content, Venus would lose most of its water post-accretion via hydrodynamic escape during a post-collision, hot water vapor atmosphere phase. The water content of all planets has likely been decreased, largely through collisional heating and subsequent hydrodynamic escape. This simple treatment assumes the water retention to be proportional to the planet's escape speed and inversely proportional to the solar flux. The mean solar flux depends on a planet's orbital distance, a , as a^{-2} . A planet's radius scales with its mass, M , as $M^{1/3}$. Thus, we assume that the water retention factor, R_{H_2O} , will scale as $R_{H_2O} \propto M^{1/3} a^2$. We adopt the following form:

$$R_{H_2O} = P1 + P2 \left(\frac{a}{1\text{AU}} \right)^2 \left(\frac{M}{1M_\oplus} \right)^{1/3}, \quad (1)$$

where $P1$ and $P2$ are parameters chosen to change the shape of the curve. $P1$ corresponds to the portion of water that avoids hydrodynamic escape, perhaps by being locked up in hydrated minerals and buried in the mantle. $P2$ is a simple scaling factor that determines the orbital radius at which R_{H_2O} reaches unity and flattens out. Figure 6 shows two cases for R_{H_2O} with different values of $P1$ and $P2$. The different curves in each panel

represent planet masses of 0.5, 1 and 2 M_\oplus . The top panel shows curve A, where $P1 = 0$ and $P2 = 0.5$, so R_{H_2O} is a very steep function that is almost directly proportional to $M^{1/3} a^2$. Water is very strongly depleted from the inner planets in this case. Curve B, shown in the bottom panel of Fig. 6, has $P1 = 0.2$ and $P2 = 0.2$, and is much shallower with 20% of water assumed to be retained on all planets. In this case, planetary water is depleted at larger radii, out to ~ 2 AU for an Earth-mass planet.

We believe our form for R_{H_2O} to be reasonable in its scaling with planet mass and orbital radius. Given the current lack of understanding, curves A and B from Fig. 6 may bracket the realistic water depletion scenarios. As seen in Fig. 3, water-rich material is not accreted by terrestrial planets until $t \sim 10$ Myr. By this time, planets have reached a significant fraction of their final masses and are generally close to their final orbital radii. It is therefore reasonable that R_{H_2O} depend only on the final mass and semimajor axis of the planet. In reality, a planet's water retention factor depends on the physical and orbital states of both bodies during and after each water-bearing impact, and the collision parameters of these impacts, throughout the history of the planet. We think that Eq. 1 is a good first approximation for the water retention of planets.

Some of the water retention values from Fig. 6 are quite small, especially for lower-mass planets close to their host star. The most extreme water depletion for any of our planets is for planet *a* from simulation 1b, a 0.6 M_\oplus planet located at 0.52 AU. Its water retention factor from curve A (curve B) is 0.11 (0.25), indicating that only about one tenth (one quarter) of its initial water remains. Table 3 lists the number of oceans of water retained by each planet assuming the water retention to follow curves A and B. For planets inside ~ 1 AU, values from curve A cause greater water depletion, but for outer planets, curve B depletes water more.

We define the equivalent ocean depth (EOD) as the depth of a global ocean on the surface of a planet, assuming the surface to be perfectly even (i.e., continent-free). The surface density of the Earth is $4\pi r_\oplus^2 = 5.11 \times 10^{18} \text{ cm}^2$. The Earth's equivalent ocean depth is simply the volume of 1 ocean ($1.5 \times 10^{24} \text{ cm}^3$) divided by its surface area, which equals 2.93 km of equivalent global ocean depth.

In calculating the amount of water on the surface of a planet, we assume the mantle to contain one ocean per 10^{27} g, as described above. For example, the mass of planet 0-*b*'s mantle is $M \times (1 - FeMF) = 1.51 M_\oplus = 8.75 \times 10^{27}$ g. By our previous arguments, planet 0-*b*'s mantle therefore contains roughly 9 oceans of water. Neglecting all volatile loss, the total water content of planet 0-*b* is 66 oceans. Using the parameters from curve B, the depletion formula from Eq. 1 indicates that only 44% of this water remains, 29 oceans. Since the iron core is thought to be devoid of water, this leaves 20 oceans on the surface of planet 0-*b*, corresponding to an equivalent global ocean depth of 37 km.

The equivalent ocean depth values in Table 3 are rather startling. Few planets have oceans with similar depths to the Earth's; most have global ocean depths much larger than the Earth's (oceans on planets beyond the habitable zone may be in the form of ice). This begs the question of whether continents can exist above the oceans on such planets. In the absence of continents, photometric variability as a function of phase would depend only on weather/cloud variability. Thus, one could not use photometric variability as a method of determining plane-

TABLE 3
PROPERTIES OF (potentially habitable) PLANETS^a

Sim.-pl.	$a(AU)$	\bar{e}^b	e_{min}, e_{max}^c	$M(M_{\oplus})$	$Rad.(km)^d$	$R_{core}(km)$	$N(oc.)A-B^e$	$EOD(km)A-B^f$
0-a	0.55	0.05	0.001, 0.11	1.54	7365	4860	3-4	0-0
0-b	0.98	0.04	0.005, 0.095	2.04	8100	4100	40-29	57-37
0-c	1.93	0.06	0.001, 0.12	0.95	6270	3100	34-31	86-79
1a-a	0.58	0.06	0.002, 0.09	0.93	6230	3180	5-8	4-13
1a-b	1.09	0.07	0.003, 0.13	0.78	5870	3000	9-7	20-13
1a-c	1.54	0.04	0.001, 0.1	1.62	7490	3690	75-57	143-105
1b-a	0.52	0.06	0.003, 0.10	0.60	5460	2800	2-4	0-7
1b-b	1.12	0.05	0.029, 0.06	2.29	8400	4390	49-32	67-37
1b-c	1.95	0.09	0.07, 0.10	0.41	4810	2315	6-5	22-15
2a-a	0.55	0.08	0.015, 0.14	1.31	6980	3770	1-1	0-0
2a-b	0.94	0.13	0.007, 0.23	0.87	6175	3150	12-11	27-22
2a-c	1.39	0.11	0.03, 0.16	1.46	7235	3745	34-22	62-35
2a-d	2.19	0.08	0.06, 0.10	1.08	6540	3180	75-75	194-194
2b-a	0.61	0.18	0.16, 0.19	2.60	8770	4580	18-21	12-17
2b-b	1.72	0.17	0.16, 0.19	1.63	7500	3830	126-113	248-221
Mercury ^g	0.39	0.19	0.13, 0.25	0.06	2436	1825	0	0
Venus	0.72	0.03	0.007, 0.07	0.82	6052	2900	1.5	0
Earth	1.0	0.03	0.000, 0.06	1.0	6378	3480	4-5	3
Mars	1.52	0.06	0.002, 0.12	0.11	3400	1700	0.1	0

^aPlanets are defined to be $> 0.2 M_{\oplus}$. Shown in bold are bodies in the habitable zone.

^bMean eccentricity averaged over the last 50 Myr of the simulation.

^cMinimum and maximum eccentricity over the last 50 Myr of the simulation.

^dPlanetary radius. We assume that planets more massive than the Earth have the Earth's bulk density, and planets less massive than the Earth have Venus' bulk density.

^eOceans of water retained by the planet through its history. The value on the left uses water retention curve A from Fig. 6, and that on the right uses curve B.

^fEquivalent ocean depth – the depth of a global ocean assuming water retention curves A and B.

^gOrbital values for the Solar system taken from Quinn *et al.* (1991). Physical values taken from Lodders & Fegley (1998). Solar system ocean and EOD values do not include estimates from curves A and B.

tary characteristics such as rotation rate (Ford *et al.* 2001).

This analysis is clearly very sensitive to our assumptions about the mantle's water capacity and the water depletion factor. We have also chosen initial conditions conducive to water delivery, in particular, Jupiter's circular orbit (Chambers & Cassen 2002; RQL04). These may, in fact, be realistic conditions for the formation of the Solar System's terrestrial planets – Tsiganis *et al.* (2005) suggest that the eccentricities of the giant planets were very low during terrestrial accretion.

In none of our simulations have we formed planets similar to Mars. This may be due in part to our relatively massive disk, which is $\sim 50\%$ more massive than the minimum mass solar nebula model. As seen in RQL04, a higher surface density increases the amount of gravitational self-stirring among protoplanets, effectively widening each planet's feeding zone and causing the planets to be more massive and fewer in number. In our simulations, however, any planets which formed past 1 AU contained a significant amount of water. Models suggest that Mars' current water budget is only 0.1 oceans, and that it only accreted water from small bodies, not embryos (Lunine *et al.* 2003). Our results are consistent in that the fraction of water accreted as embryos vs. planetesimals decreases with planetary mass. However, all planets in our simulations outside the habitable zone accreted at least 5 oceans of water. The solution may lie with water retention, as Mars' water content was likely much higher in the past. Perhaps water retention during accretion is a stronger function of planetary mass than shown in Eq. 1.

Mars' small size remains unexplained. Its proximity to the ν_6 secular resonance with Saturn at 2.1 AU could have caused high-velocity, potentially erosional impacts as seen in Agnor & Asphaug (2004). However, a recent model suggests that the gi-

ant planets did not reach their final configuration until ~ 700 Myr (Tsiganis *et al.* 2005). In this context, ν_6 resonance may not have existed during Mars' accretion. Its small size may have more to do with the direct influence of Jupiter, and could imply a rapid formation of Jupiter.

4.2. Moon-forming impacts

The Earth owes much of its stability to the Moon. Without the Moon, the Earth's obliquity would vary chaotically between zero and 85 degrees (Laskar *et al.* 1993). It is unclear whether high-obliquity, Earth-like planets would be habitable, but the effects on the climate would certainly be drastic (e.g., Williams & Pollard, 2003).

The Earth's moon is thought to have formed from re-accumulation of material after the oblique impact of a roughly Mars-sized body (e.g., Canup & Asphaug, 2001). This impact may have occurred relatively late in the Earth's accretion history, because the Moon would have difficulty surviving tens of Myr of accretion, although opposing viewpoints exist (see Canup, 2004, for a review). A moon-forming impact needs to deliver sufficient angular momentum to form a massive circumplanetary disk from which a moon can accrete. Such a collision must therefore be off-center. However, grazing collisions do not form moons, but rather may erode both bodies (Agnor & Asphaug, 2004).

If large moons are preferentially formed in the last stages of accretion, Fig. 3 suggests that many such impactors may originate past the snow line and also deliver water. However, isotopic constraints imply that the Earth and Moon formed at roughly the same orbital radius (see, e.g., Canup 2004). Belbruno & Gott (2005) propose that the proto-Moon may have accreted in a 1:1 resonance with the Earth, at either the L4 or

L5 Lagrangian points. After some time, the proto-Moon was scattered by other growing protoplanets onto an Earth-crossing orbit. This scenario predicts a low relative velocity impact, as needed to form the Moon. Our results are consistent with this scenario. Figure 3 shows that planetary feeding zones widen in time. At late times (after ~ 10 Myr), the starting location of giant impactors may be anywhere in the terrestrial region. Several late impacts come from past 2.5 AU and are therefore water-rich, but some originate very close to the planets' final positions.

4.3. Habitability of simulation planets

Planet 0-*b* (planet *b* from simulation 0) is potentially habitable. Its semimajor axis lies at the inner edge of the habitable zone, which we define to lie between 0.9 and 1.4 AU. Planet 0-*b*'s mean eccentricity of 0.04 is small enough that its perihelion lies just outside the inner edge of the habitable zone, at 0.94 AU. However, the time-averaged eccentricity does not capture fluctuations over Myr timescales. From 150–200 Myr, planet 0-*b*'s minimum and maximum eccentricity were 0.005 and 0.095, respectively. In its high eccentricity state, its perihelion is 0.89 AU, just inside the inner edge of the habitable zone.

Planet 1a-*b* and 1b-*b* also lie in the habitable zone and have significant water contents, although planet 1b-*b* is much more massive. Planet 1a-*b*'s orbital radius is 1.09 AU, and its mean, time-averaged eccentricity is 0.07, although it can reach 0.13 over long timescales. In such high-eccentricity periods, its perihelion approaches the inner edge of the habitable zone, at 0.95 AU. Planet 1b-*b*'s semimajor axis is 1.12 AU and its mean eccentricity is 0.046, but varies from 0.029 to 0.06 over 10 Myr timescales. Its orbit never leaves the habitable zone, with extreme perihelion of 1.05 AU and extreme aphelion of 1.19 AU.

A very interesting case is simulation 2a, which formed two planets in the habitable zone. Planet *b* lies at the inner edge, at 0.94 AU. Planet *c* skirts the outer edge of the habitable zone, at 1.39 AU. The eccentricities of both planets vary by significant amounts over Myr timescales. Like planet *b* from simulation 0, their orbits do not remain in the habitable zone at all times. The eccentricities of planets *b* and *c* from simulation 2a are interdependent; when planet *b* is in a high-*e* state, planet *c* is in a low-*e* state, and vice versa. Figure 7 shows the eccentricity evolution of the two planets as a function of time for a 2 Myr interval late in the simulation. The amplitude of planet *b*'s eccentricity variation is larger than planet *c*'s, and the variations of each planet are exactly out of phase. In fact, planets *b* and *c* are in a *secular resonance* – over long timescales the orientation of their orbits librate about anti-alignment. Figure 8 shows the distribution function of Λ , the difference between the longitudes of pericenter of planets *b* and *c*, constrained to lie between 0 and 180 degrees (Barnes & Quinn 2004). At no point during the final 50 Myr of the simulation does Λ have a value less than 90 degrees. $P(\Lambda)$ peaks at $\Lambda \approx 110$ –120°, then tails off at higher values. This indicates that the amplitude of libration about anti-alignment ($\Lambda = 180^\circ$) is 60–70°.

Figure 9 shows the orbits of planets *b* (in red) and *c* (in blue) from simulation 2a at two different times. During time 1 (left panel), planet *b*'s eccentricity is low and planet *c*'s is high, and during time 2 (right panel), planet *b*'s eccentricity is high and planet *c*'s is low. Fig. 9 shows the most extreme eccentricities values found for the planets over the last 50 Myr of the simulation, to show the range of orbits. The anti-alignment of longitudes of pericenter is evident as planet *b*'s perihelion at time 2 is on the opposite side of the Sun from planet *c*'s perihelion at

time 1.

At time 1, planet *b*'s orbit stays at the inner edge of the habitable zone, but planet *c* strays far past the outer edge, to its aphelion of 1.61 AU. At time 2, planet *b* ventures far inside the inner edge of the habitable zone, with a perihelion distance of 0.73 AU, while planet *c* skirts the outer edge of the habitable zone. During episodes of high eccentricity, the time-averaged distance d of planet *b* from its host star, $d = a(1+e^2/2)$, remains in the habitable zone. A higher eccentricity increases a planet's time-averaged distance, simply because a planet's orbital velocity decreases with orbital distance. A higher eccentricity does, of course, cause greater extremes. If, at perihelion, planet *b* is sufficiently heated that it loses some of its water, then over time its water content could evaporate. However, spending a larger time-averaged fraction of its orbit far from the star might counteract the increased heating at perihelion. During times of high eccentricity, planet *c*'s time-averaged orbital radius is increased to 1.41 AU, just beyond the habitable zone. Over the course of an orbit, water on its surface may alternately freeze and thaw. Williams & Pollard (2002) find that the more important quantity for climate stability is the mean stellar flux received on the planetary surface, rather than the time spent in the habitable zone. Detailed models of orbit-climate interaction (e.g. Williams & Pollard 2002, 2003; Armstrong *et al.* 2004) are needed to assess the habitability of such planets.

4.4. Discussion of planetary habitability

Water is thought to be an essential ingredient for both life and the physical properties of a planet. Water lowers the viscosity of rocks, and may be an important factor in determining whether a planet will develop plate tectonics (Regenauer-Lieb, 2001). Plate tectonics, in turn, plays an essential role in climate stabilization through the carbon cycle. The large water contents of the planets are not unexpected, since our initial conditions contain about 50% more mass than the minimum mass solar nebula (e.g., Hayashi 1981) and only one giant planet on a circular orbit. An eccentric giant planet or simply an additional giant planet would increase the magnitude of Jupiter's secular perturbations and would tend to scatter water-rich protoplanets out of the planetary system rather than allowing them to diffuse inward and deliver water to the terrestrial planets (Chambers & Cassen 2002; Levison & Agnor 2003; RQL04).

Lissauer (1999) outlined the general properties of potentially habitable planets with different masses. A planet smaller than the Earth probably has a lower surface gravity, so it is likely to lose more volatiles to space (as seen in Eq. 1 and Fig. 6), and also to have higher mountains (and deeper valleys) than the Earth. The planet's higher surface area to volume ratio allows it to cool faster. A small planet's atmospheric pressure is likely to be smaller, with less greenhouse effect, leading to a cooler surface. Conversely, a larger planet than the Earth cools more slowly and has a higher surface gravity with flatter topography. It would have a higher atmospheric pressure and surface water content, possibly covering the surface in a global ocean.

Lissauer (1999) suggests that smaller planets have a higher chance of being habitable if they lie closer to the Sun and have higher concentrations of volatiles and radioactive elements. Larger planets may be more habitable farther from the Sun with fewer volatiles, to enable the existence of continents. This speculated widening of the habitable zone could mean that planets 1b-*c* and 2b-*b* are suitable for life.

5. CONCLUSIONS

We have investigated water delivery and planetary habitability in five simulations with roughly an order of magnitude more particles than in previous work (Paper 1). The planets that formed in these simulations were qualitatively similar to those formed in previous simulations, except that *every single* planet we formed was delivered at least five Earth oceans of water. We form many planets with a large amount of water, reminiscent of “water world” planets formed in RQL04. Léger *et al.* (2004) investigated the interior structure of such planets.

The feeding zones of the terrestrial planets widen and move outward in time, as shown in Fig. 3. Assuming embryos to form slowly (as in Kokubo & Ida 2000), planets do not accrete water-rich material until at least 10 Myr after the start of a simulation, at which time most planets are a sizable fraction of their final mass.

The stochasticity of the water delivery process in previous simulations has been overestimated (Morbidelli *et al.*, 2000; RQL04). The accretion of water-rich material was thought to be a “hit or miss” process, implying that many Earth-like planets would be devoid of water (at least from a chondritic source). Here we have shown that a significant fraction of the water delivered to terrestrial planets is in the form of planetesimal-sized

bodies. A planet will accrete a large amount of water in the form of a few large embryos in a “hit or miss” process. In addition, a planet will accrete at least two oceans (and up to ≥ 20) of water from a large number of smaller bodies in a statistically robust way. The dynamics of these small bodies differ from that of embryos’, though simulations of 10^9 planetesimals are not currently feasible. The water from small bodies is likely to be retained, but the retention of water during large impacts is less certain. We therefore expect that terrestrial planets in the Galaxy will have a range of water contents, but the range will be less than previously thought (RQL04).

The stochasticity or robustness of water delivery appears to depend strongly on the formation timescale of planetary embryos between 2.5 and 4 AU. If embryos form quickly (Goldreich *et al.* 2004), then the number of bodies involved in water delivery is relatively small, and the process is relatively stochastic (although far less than in previous models – Morbidelli *et al.* 2004, RQL04). However, if embryos form more slowly (Kokubo & Ida 2000, 2002; Leinhardt & Richardson 2005), then the number of water-bearing impactors is larger. In this scenario, water delivery is an even more robust process.

REFERENCES

Agnor, C., & Asphaug, E. 2004. Accretion Efficiency during Planetary Collisions. *ApJ*, 613, L157.

Armstrong, J. C., Leovy, C. B., & Quinn, T. 2004. A 1 Gyr climate model for Mars: new orbital statistics and the importance of seasonally resolved polar processes. *Icarus*, 171, 255.

Barnes, R., & Quinn, T. 2004. The (In)stability of Planetary Systems. *ApJ* 611, 494-516.

Belbruno, E., & Gott, J. R. I. 2005. Where did the Moon come from? *AJ*, 129, 1724.

Boss, A. P. 1997. Giant planet formation by gravitational instability. *Science* 276, 1836.

Briceño, C., Vivas, A. K., Calvet, N., Hartmann, L., Pacheco, R., Herrera, D., Romero, L., Berlind, P., Sanchez, G., Snyder, J. A., Andrews, P., 2001. The CIDA-QUEST Large-Scale Survey of Orion OB1: Evidence for Rapid Disk Dissipation in a Dispersed Stellar Population. *Science* 291, 93-97.

Canup, Robin M., Asphaug, Erik 2001. Origin of the Moon in a giant impact near the end of the Earth’s formation. *Nature*, 412, 708-712.

Canup, R. M. 2004. Dynamics of Lunar Formation. *Annual Reviews of Astron. & Astrophys.*, 42, 441

Chambers, J. E., 1999. A Hybrid Symplectic Integrator that Permits Close Encounters between Massive Bodies. *MNRAS*, 304, 793-799.

Chambers, J. E. & Cassen, P., 2002. The effects of nebula surface density profile and giant-planet eccentricities on planetary accretion in the inner Solar system. *Meteoritics and Planetary Science*, 37, 1523-1540.

Cyr, K. E., Sears, W. D., & Lunine, J. I. 1998. Distribution and Evolution of Water Ice in the Solar Nebula: Implications for Solar System Body Formation. *Icarus*, 135, 537

Drake, M. J. and Righter, K., 2002. What is the Earth made of? *Nature* 416, 39-44.

Ford, E. B., Seager, S., & Turner, E. L. 2001. Characterization of extrasolar terrestrial planets from diurnal photometric variability. *Nature*, 412, 885-887

Genda, H., & Abe, Y. 2003. Survival of a proto-atmosphere through the stage of giant impacts: the mechanical aspects. *Icarus*, 164, 149

Genda, H., & Abe, Y. 2005. Enhanced atmospheric loss on protoplanets at the giant impact phase in the presence of oceans. *Nature*, 433, 842

Goldreich, P., Lithwick, Y., & Sari, R. 2004. Final Stages of Planet Formation. *ApJ*, 614, 497

Gomes, R., Levison, H. F., Tsiganis, K., & Morbidelli, A. 2005. Origin of the cataclysmic Late Heavy Bombardment period of the terrestrial planets. *Nature*, 435, 466

Hayashi, C. 1981. Structure of the solar nebula, growth and decay of magnetic fields and effects of magnetic and turbulent viscosities on the nebula. *Prog. Theor. Phys. Suppl.*, 70, 35-53.

Kasting, J. F., Whitmire, D. P., and Reynolds, R. T., 1993. Habitable zones around main sequence stars. *Icarus* 101, 108-128.

Kokubo, E., & Ida, S., 2000. Formation of Protoplanets from Planetesimals in the Solar Nebula. *Icarus* 143, 15-27.

Kokubo, E., & Ida, S., 2002. Formation of Protoplanet Systems and Diversity of Planetary Systems. *ApJ* 581, 666.

Laskar, J., Joutel, F., & Robutel, P. 1993. Stabilization of the earth’s obliquity by the moon. *Nature*, 361, 615

Léger, A., Selsis, F., Sotin, C., Guillot, T., Despous, D., Mawet, D., Ollivier, M., LabAíque, A., Valette, C., Brachet, F., Chazelas, B., Lammer, H. 2004. A new family of planets? “Ocean-Planets”. *Icarus* 169, 499-504.

Leinhardt, Z. M., & Richardson, D. C. 2005. Planetesimals as Protoplanets. I. Effect of Fragmentation on Terrestrial Planet Formation. *ApJ*, 625, 427

Levison, H. F. & Agnor, C., 2003. The Role of Giant Planets in Terrestrial Planet Formation. *AJ*, 125, 2692-2713.

Lissauer, J. J. 1993. Planet Formation. *ARAA*, 31, 129.

Lissauer, J. J. 1999. How common are habitable planets? *Nature* 402, C11-C14.

Lodders, K., & Fegley, B. 1998, The planetary scientist’s companion. Oxford University Press, 1998.

Lunine, J. I., Chambers, J., Morbidelli, A. and Leshin, L. A., 2003. The origin of water on Mars. *Icarus*, 165, 1-8.

Matsu, T. & Abe, Y. 1986. Impact-induced atmospheres and oceans on earth and Venus. *Nature* 322, 526

Morbidelli, A., Chambers, J., Lunine, J. I., Petit, J. M., Robert, F., Valsecchi, G. B., and Cyr, K. E., 2000. Source regions and timescales for the delivery of water on Earth. *Meteoritics and Planetary Science* 35, 1309-1320.

Pollack, J. B., Hubickyj, O., Bodenheimer, P., Lissauer, J. J., Podolak, M., & Greenzweig, Y., 1996. Formation of the Giant Planets by Concurrent Accretion of Solids and Gas. *Icarus*, 124, 62-85.

Quinn, Thomas R., Tremaine, Scott, & Duncan, Martin, 1991. A three million year integration of the earth’s orbit. *AJ* 101, 2287-2305.

Raymond, S. N., Quinn, T., & Lunine, J. I., 2004. (RQL04) Making other earths: dynamical simulations of terrestrial planet formation and water delivery. *Icarus*, 168, 1-17.

Raymond, S. N., Quinn, T., & Lunine, J. I. 2005a. The formation and habitability of terrestrial planets in the presence of close-in giant planets. *Icarus*, 177, 256-263.

Raymond, S. N., Quinn, T., & Lunine, J. I. 2005b. Terrestrial Planet Formation in Disks with Varying Surface Density Profiles. *ApJ*, 632, 670-676.

Raymond, S. N., Quinn, T., & Lunine, J. I. 2006. (Paper 1) High-resolution simulations of the final assembly of Earth-like planets 1: terrestrial accretion and dynamics. *Icarus*, submitted, astro-ph/0510284

Regenauer-Lieb, K., Yuen, D. A., & Branhund, J. 2001. The initiation of subduction: Criticality by addition of water? *Science* 294(5542): 578-580.

Segura, T. L., Toon, O. B., Colaprete, A., & Zahnle, K. 2002. Environmental Effects of Large Impacts on Mars. *Science*, 298, 1977

Sleep, N. H., & Zahnle, K. 1998. Refugia from asteroid impacts on early Mars and the early Earth. *JGR*, 103, 28529

Tsiganis, K., Gomes, R., Morbidelli, A., & Levison, H. F. 2005. Origin of the orbital architecture of the giant planets of the Solar System. *Nature*, 435, 459

Weidenschilling, S. J., Spaute, D., Davis, D. R., Marzari, F., & Ohtsuki, K. 1997. Accretional Evolution of a Planetesimal Swarm. *Icarus*, 128, 429

Wetherill, G. W., 1996. The Formation and Habitability of Extra-Solar Planets. *Icarus*, 119, 219-238.

Williams, D. M., Kasting, J. F., & Wade, R. A. 1997. Habitable moons around extrasolar giant planets. *Nature*, 385, 234-236.

Williams, D. M., & Pollard, D. 2002. Earth-like worlds on eccentric orbits: excursions beyond the habitable zone. *International Journal of Astrobiology*, 1, 61.

Williams, D. M., & Pollard, D. 2003. Extraordinary climates of Earth-like

planets: three-dimensional climate simulations at extreme obliquity. International Journal of Astrobiology, 2, 1-19

Zahnle, K. 2005. Planetary science: Being there. Nature, 433, 814

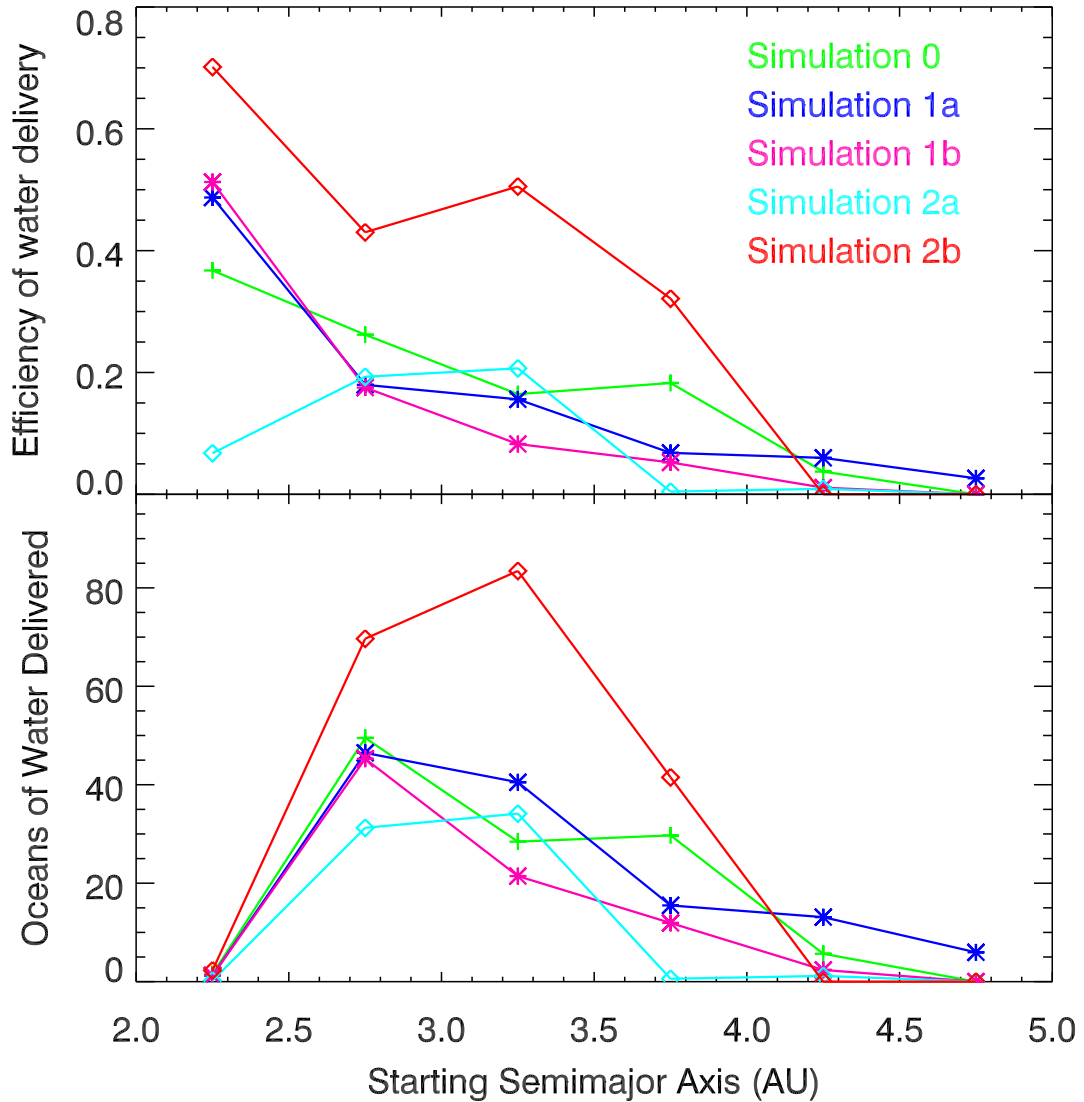


Fig. 1.— Top: Efficiency of water delivery in each of our five simulations. Each point represents the fraction of the (water-rich) material in a given 0.5 AU-wide bin to have been delivered to the surviving terrestrial planets inside 2 AU. Bottom: Source of water for the terrestrial planets in each simulation. Each point shows the number of oceans of water delivered from a given 0.5 AU-wide region to the surviving terrestrial planets inside 2 AU. Planet *d* from simulation 2a is not included in either panel.

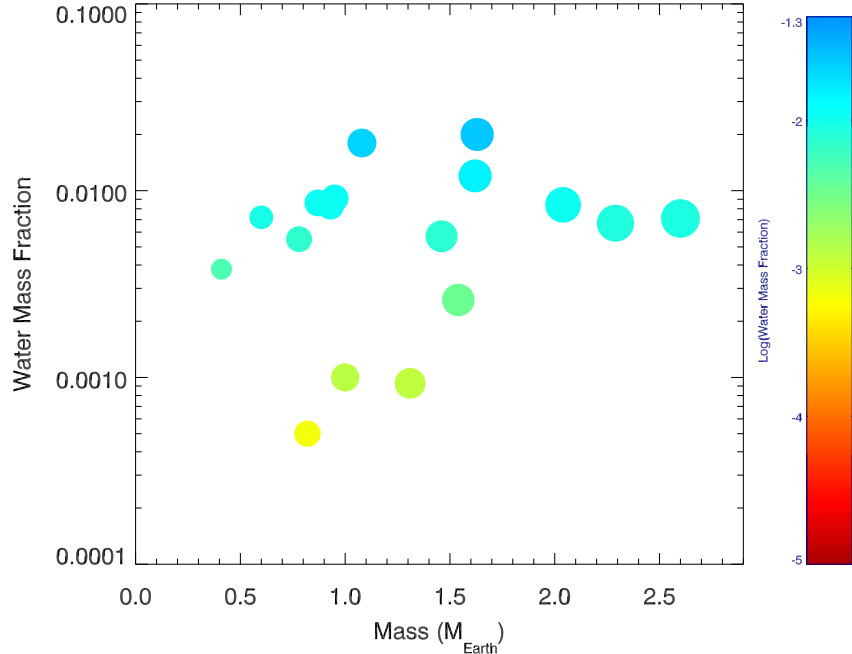


Fig. 2.— Water mass fraction of the surviving terrestrial planets as a function of their final mass. The size of each body is proportional to its relative physical size. The color of each body corresponds to its water mass fraction, as shown in the color bar on the right for values from 10^{-5} (red) to 0.05 (blue).

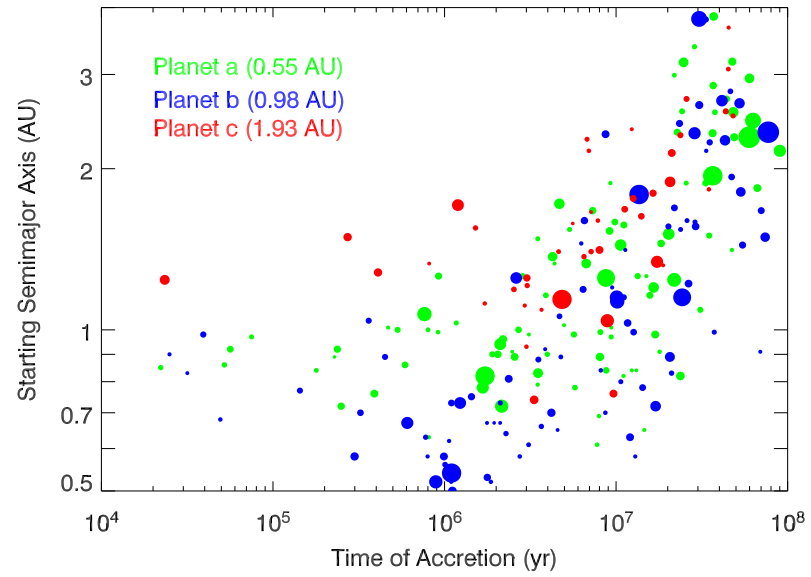


Fig. 3.— The timing of accretion of bodies from different initial locations for simulation 0. All bodies depicted in green were accreted by planet *a*, all blue bodies were accreted by planet *b*, and all red bodies were accreted by planet *c*. The relative size of each circle indicates its actual relative size. Impactors which had accreted other bodies are given their mass-weighted starting positions. Reproduced from Paper 1.

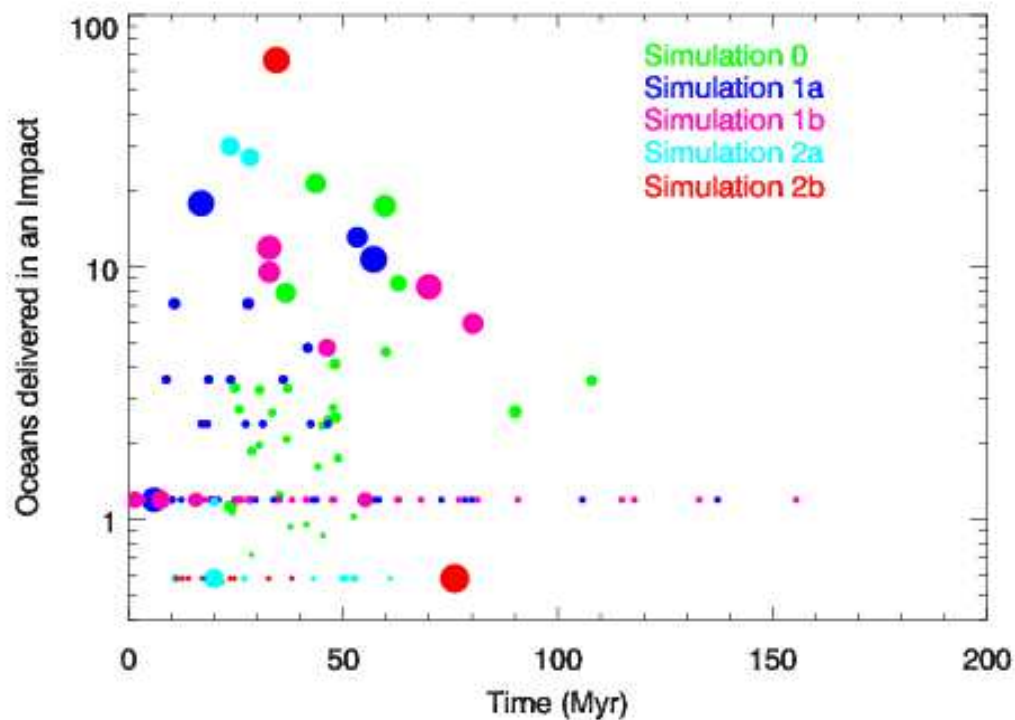


Fig. 4.— The amount of water (in units of Earth oceans) delivered to the terrestrial planets in each impact, shown through time. The size of each point represents the relative physical size of the impactor. The water contained in a planetesimal in simulations 1a and 1b is evident.

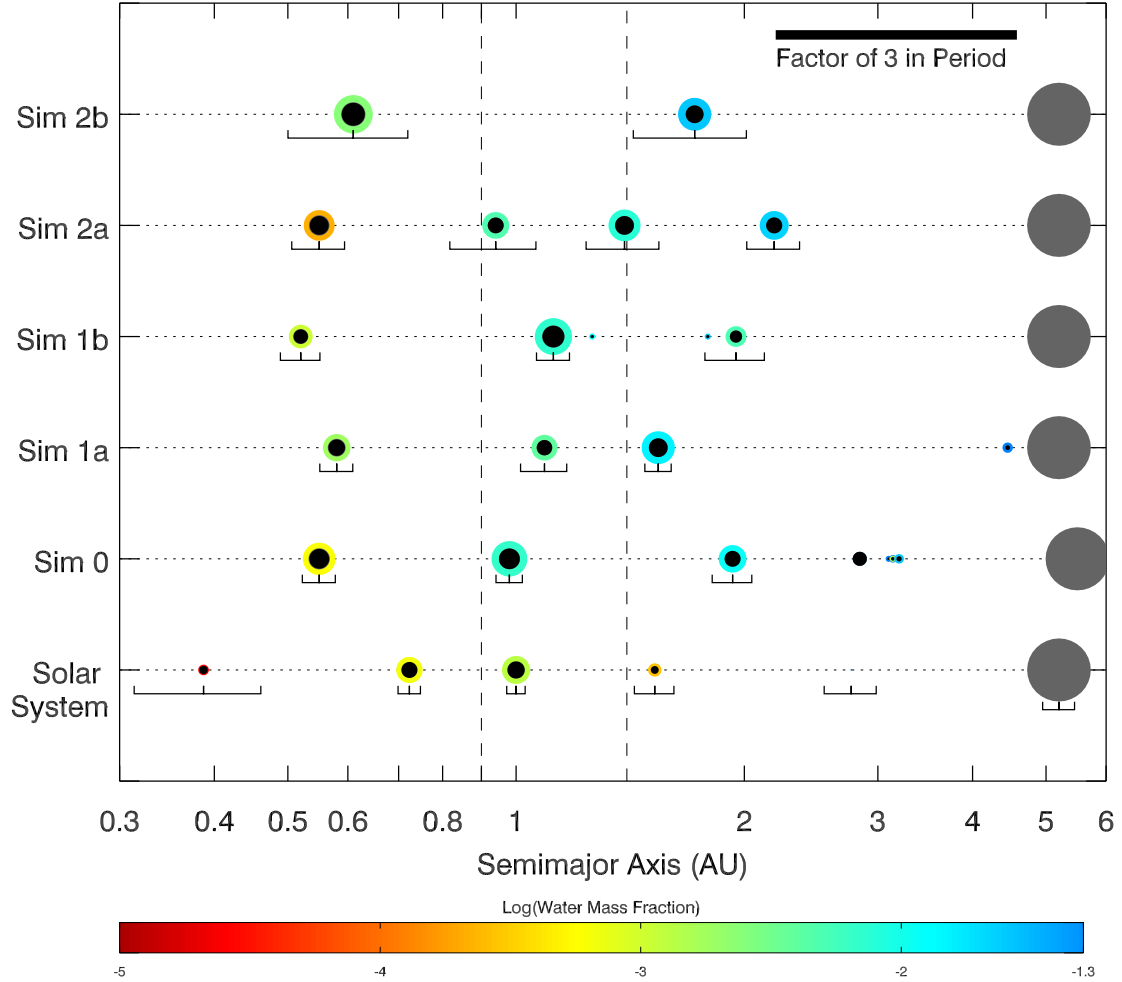


Fig. 5.—Final configurations of all five high-resolution simulations, with the Solar system (including the largest asteroid, Ceres) shown for scale. The x axis is on a log scale, such that a fixed distance corresponds to a fixed ratio of orbital periods – the scale bar in the upper right shows a factor of three in period. The relative size of each body corresponds to its relative physical size. The color of each body represents its water mass fraction, including an assumed depletion following curve A from Fig. 6. The vertical dashed lines represent the inner and outer boundaries of the habitable zone.

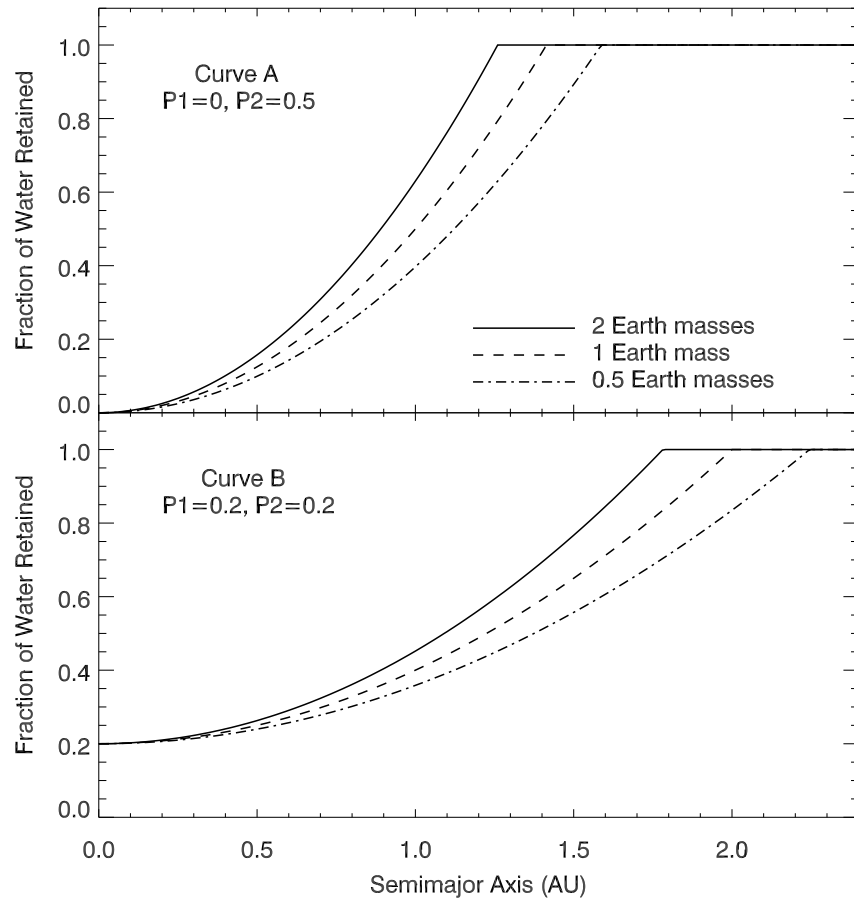


Fig. 6.— The fraction of water retained (R_{H_2O} in the text) as a function of semimajor axis, shown for three different planet masses. Curve A is shown in the top plot, with parameters from Eq.1 of $P1 = 0$, $P2 = 0.5$. Curve B is shown in the bottom plot, with $P1 = 0.2$, and $P2 = 0.2$.

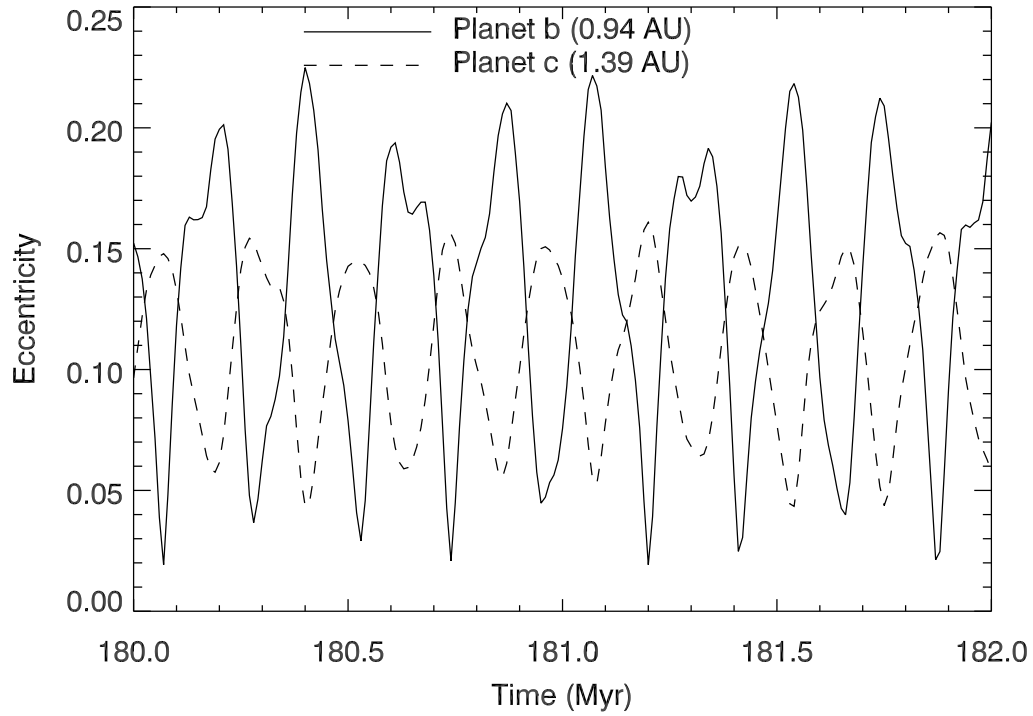


Fig. 7.— Eccentricities of planets b and c from simulation 2a as a function of time, toward the end of the simulation.

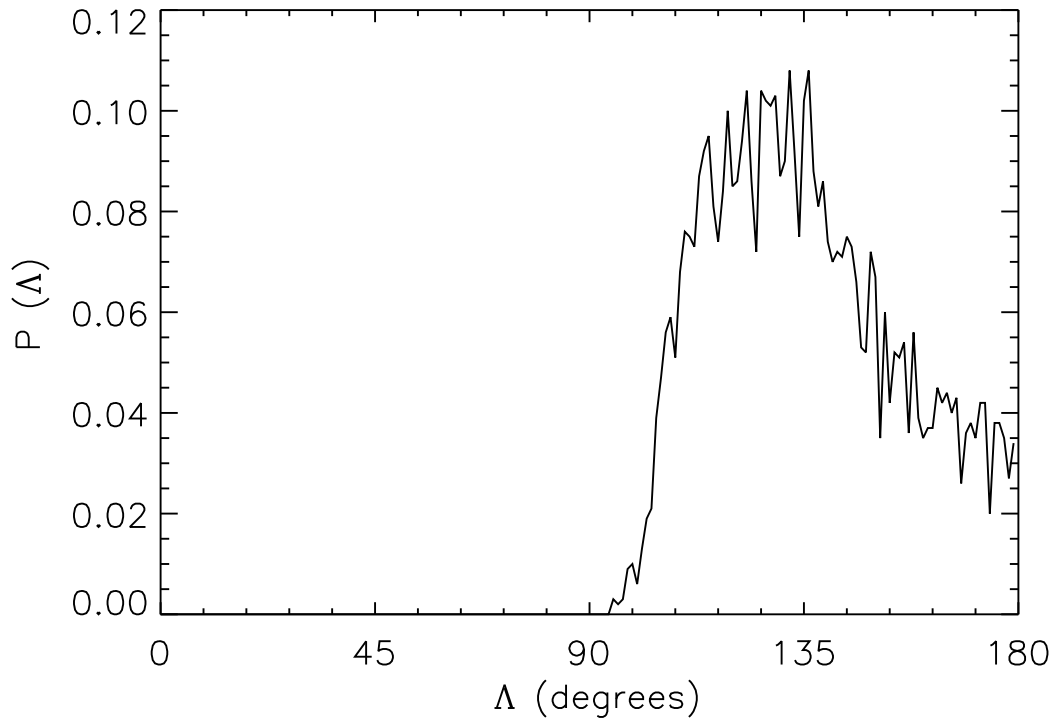


Fig. 8.— Distribution function, $P(\Lambda)$, of the relative alignment of the longitudes of pericenter, Λ , of planets b and c from simulation 2a. The longitudes are librating about anti-alignment ($\Lambda = 180^\circ$).

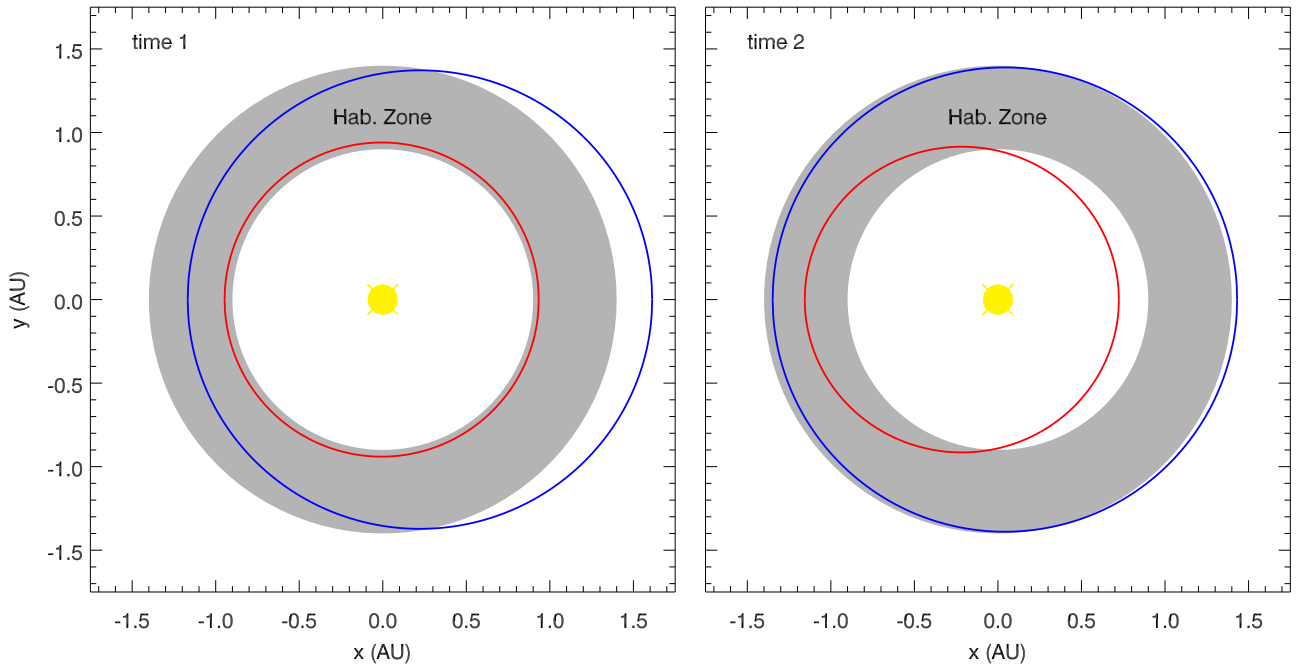


Fig. 9.— The orbits of planets b (red) and c (blue) from simulation 2a at two different times. During time 1 (left panel), planet b 's eccentricity is low and planet c 's is high. During time 2 (right panel), roughly 100 kyr after time 1 (see Fig. 7), planet b 's eccentricity is high and planet c 's is low. The habitable zone between 0.90 and 1.40 AU is shaded. The Sun is shown in yellow at the origin (not to scale).